JOURNAL OF AGRICULTURAL AND FOOD CHEMISTRY

Adsorption of Atrazine, Hydroxyatrazine, Deethylatrazine, and Deisopropylatrazine onto Fe(III) Polyhydroxy Cations Intercalated Vermiculite and Montmorillonite

GILBERTO ABATE* AND JORGE CESAR MASINI

Instituto de Química, Universidade de São Paulo, CP 26077, 05513-970 São Paulo, SP, Brazil

This paper describes the modification of the clay minerals vermiculite (VT) and montmorillonite (MT) by intercalating Fe(III) polymers of different [OH^-]:[Fe(III)] ratios with the aim of removing atrazine (AT) and its metabolites deethylatrazine (DEA), deisopropylatrazine (DIA), and hydroxyatrazine (ATOH) from aqueous solution. An enhancement of adsorption capacity was observed for both intercalated clay minerals in comparison to the potassium-saturated materials (KVT or KMT). The results showed that different [OH^-]:[Fe(III)] molar ratios had a small influence on the adsorption capacity, as well as in the basal spacing, BET surface area, and porosity. For the lowest initial concentrations of AT, DIA, and ATOH (0.050 mg L^{-1}) studied, the modified VT adsorbed almost 80% of AT and DIA, while ATOH was removed at concentration levels below the detection limit of the technique, implying in at least 99.5% of sorption. Weak interaction between intercalated VT and DEA was observed, although a significant adsorption enhancement occurred in comparison to KVT. Within a 24 h interval, desorption of AT and DIA in aqueous medium reached levels close to 20% of the amount initially adsorbed, while for ATOH only 3% of the adsorbed compound was desorbed. The adsorption capacity of the Fe(III)-intercalated VT decreased after the first adsorption/desorption cycle, implying that the material is not suitable for reutilization. The intercalated MT was a powerful sorbent for AT, DEA, DIA, and ATOH, removing all of these chemicals from solution almost quantitatively (sorption greater than 99.5%), even at initial concentrations as high as 1.0 mg L^{-1}. Additionally, desorption of AT, ATOH, and DIA in water was not measurable up to the tube corresponding to the initial concentration of 1.0 mg L^{-1}, suggesting strong irreversible binding of these compounds to the intercalated MT materials. Desorption of DEA from the intercalated MT was between 5 and 30%. Unlike what was observed for VT, the intercalated MT materials were recyclable, keeping an excellent performance when reutilized.

KEYWORDS: Atrazine; atrazine metabolites; intercalated clays; adsorption

INTRODUCTION

Increasing agricultural productivity has caused environmental problems related to the large use of agrochemicals, especially herbicides. The contamination of soils, groundwater, and surface water by herbicides is a concern of prime importance due to the serious effects that these compounds have on humans and other animals, as well as on the equilibrium of ecosystems (*1*). Atrazine [2-chloro-4-(ethylamino)-6-isopropylamine-s-triazine, AT] is one of the most largely applied herbicides in several crops such as sugar cane, maize, soybean, and citrus fruits (*1*). Although AT is not an extremely harmful herbicide, it interacts weakly with soil components, having a high geochemical mobility, a behavior that implies easy leaching and groundwater contamination (*2*, *3*). Biotic processes facilitate the degradation of AT to produce the dealkylated metabolites deethylatrazine (DEA), deisopropylatrazine (DIA), and didealkylatrazine (DDA), while chemical hydrolysis leads to formation of hydroxyatrazine (ATOH) (*4*, *5*). AT and the dealkylated metabolites have similar physicochemical properties such as water solubility, high polarity, low degree of adsorption in soils, and high persistence, often being detected in groundwaters. Conversely, ATOH interacts strongly with clay minerals and humic substances, preferentially being retained in soils (*6*). AT metabolites have also toxicological effects (*7*), especially DEA, which is considered as phytotoxic as AT (*1*). These characteristics have driven several efforts to investigate the presence and behavior of AT in soils (*2*, *5*, *6*, *8*, *9*) and waters (*10*−*13*).

Clays and modified clay minerals properties such as small particle size, high external superficial area, high adsorption capacity, low cost, and ready availability can be exploited to develop materials and technologies to minimize the runoff and leaching of pesticides (*14*). Some of these materials have found technological applications such as herbicide formulations with controlled releasing of active components in the soil (*14*−*16*), cleanup of contaminated soils, groundwater protection (*17*, *18*),

* To whom correspondence should be addressed. Fax: 55 11 3815-5570. E-mail: gilbertoabate@ig.com.br.

10.1021/jf048556j CCC: $30.25
Published on Web 02/05/2005

and water treatment (*19*−*24*). Intercalating and pillaring are the most important interlamelar modifications of clay minerals for environmental applications. These modifications consist of exchanging the interlayer cation (K^+, Na^+, and Ca^{2+}) by a polynuclear hydroxyl metal cation (intercalating), followed by thermal treatment to obtain a series of oxide pillars between the layers of the clay mineral structure (*25*). The Al_{13} oligomer is the intercalating/pillaring agent most frequently used, with a Keggin structure and formulas of $[Al_{13}O_4(OH)_{24}(H_2O)_{12}]$ (*23*). Indeed, all metal cations that form polynuclear species can be used as intercalating or pillaring agents, for instance, Zr^{3+}, Cr^{3+}, Fe^{3+}, and Ti^{3+} (*26*). Intercalating and pillaring increase the basal spacing d(001), the specific surface area, and the microporosity of the clay mineral (*27*, *28*). The characteristics of the synthesized materials are strongly influenced by experimental parameters such as the $[OH^-]$:$[M^{x+}]$ molar ratio, reaction temperature, time, and temperature of aging, nature of the counterion, and the relative amount of the polycation to clay mineral (*26*).

Aluminum- and Fe-pillared clays exhibit high affinity by herbicides such as AT, propazine, prometryne, propachlor, propanil, and molinate (*21*). This is explained by the protonation of the compounds in the interlayer waters of the clay mineral as a consequence of the high acidity generated by the hydrolysis of the trivalent cations, leading to adsorption processes governed by cation exchange and/or electrostatic interactions. Similar processes have been observed for other weakly basic herbicides such as the hexazinone (*16*). Matthes and Kahr (*22*) demonstrated that Al- and Zr-pillared bentonites are very efficient materials to adsorb the organic bases 3-chloroaniline and AT from aqueous media. Both Al- and Zr-pillared bentonites were also able to adsorb the acid 3-chlorophenol from aqueous solution, although to a lesser extension in comparison to organic bases. These findings suggest that intercalated and pillared clays with high acidity may be used for removal of other organic bases.

This paper describes the modification of vermiculite (VT) and montmorillonite (MT) by intercalating Fe(III)−hydroxy polymeric species, with the aim of removing low concentrations of AT, DEA, DIA, and ATOH from aqueous media. The adsorption properties of the parent herbicide AT on both intercalated and pillared clays such as MTs and bentonites (*21*, *22*) have been studied, but no information about its main metabolites has been reported in the literature. DEA is the metabolite of major concern because it is as phytotoxic as AT, interacting very weakly with soil components, and it is easily leached to groundwaters. VT has several commercial mines around the world, but to our knowledge, no studies reporting the adsorption of triazines onto this clay mineral have been described. Therefore, the adsorption properties of modified VT are very important, not only for the chemicals studied here but also for other pollutants.

MATERIALS AND METHODS

Materials and Reagents. The VT clay was supplied by Eucatex Química e Mineral Ltda, from the Massapê mine located in Paulistana, PI, Brazil, with grains <1 mm. The acid-activated MT clay (K10, 28152-2) and anhydrous iron chloride were purchased from Aldrich. The analytical standards of AT, DEA, DIA, and ATOH were supplied by Riedel-de Haën. Stock solutions (1000 mg L^{-1}) were prepared in methanol [high-performance liquid chromatography (HPLC) grade]. ATOH was previously dissolved in 1 mL of 1.0 mol L^{-1} HCl solution and diluted with methanol. These standards, solids, or solutions were stored in freezer at −18 °C. Acetonitrile (ACN) and methanol (HPLC grade) were purchased from JT Baker. Water used in all experiments was distilled and deionized using the NANOpure II (Sybron Barnstead) system. All other reagents used in this work were of analytical grade from Merck or similar.

Equipment. A LC 9A Shimadzu HPLC, equipped with a SPD 6 AV UV detector, and the LC Workstation Class-LC 10 software were used in all experiments for separation and quantification of AT and their metabolites. A SB C-18 Zorbax-HP column (3.5 μm, 150 mm × 4.6 mm) connected to a C-18 Phenomenex guard column was used. Sample injection was made with a rotary Rheodyne valve using a 20 μL sample loop. A Metrohm 654 potentiometer (precision of 0.1 mV or 0.001 units of pH), coupled to an Ag/AgCl combination glass electrode, was utilized for all of the pH measurements.

Preparation of the Clay Minerals. The VT was ground, and the fraction between 0.27 and 56 μm was separated by decantation as described elsewhere (*29*). Approximately 15 g of VT or MT was treated with 0.05 mol L^{-1} HCl under agitation in a horizontal shaker for 30 min in order to obtain the proton-saturated forms of the clays, eliminating the weakly bound alkaline and earth alkaline metal cations. The solid phases were centrifuged, washed with 80 mL of deionized water, and then equilibrated with 50 mL of 1.0 mol L^{-1} KCl solution for 30 min. The solid phases were separated by centrifugation and treated a second time with 50 mL of 1.0 mol L^{-1} KCl solution for another period of 30 min in order to obtain the K^+ homoionic clay mineral (denoted by KVT and KMT for VT and MT, respectively). Finally, the excess of KCl was eliminated by washing the solid phases with deionized water, which was separated by centrifugation. Both clay minerals were dispersed in approximately 100 mL of deionized water, and the concentration of these stock suspensions was determined by the dry weight of 1.00 mL of homogenized aliquots, resulting 139 and 160 g L^{-1} for KVT and KMT, respectively. The cation exchange capacity (CEC) was determined by the method of sodium saturation (*30*), with resulting values of 1.17 ± 0.01 and 0.59 ± 0.01 mmol g^{-1} for KVT and KMT, respectively.

Intercalated Clays. The first step is the preparation of the intercalating Fe(III) suspension, which was made by adding 50 mL of 0.8 mol L^{-1} NaOH solution to 50 mL of 0.4 mol L^{-1} $FeCl_3$ with a flow rate of 1.0 mL min^{-1} using a peristaltic pump. The reaction medium was maintained under stirring while the NaOH solution was pumped, providing a 2:1 molar ratio of $[OH^-]$:[Fe(III)]. The solution was maintained at 50 °C for 48 h. Next, the KVT and KMT suspensions were heated at 50 °C, and the intercalating solution was added at a flow rate of 1.0 mL min^{-1} under strong stirring, providing a ratio of 10 mmol of Fe(III) per gram of clay minerals. The suspensions were left to rest for 72 h.

The KVT suspension was also treated by intercalating solutions suspensions with 0.75:1, 1:1, and 1.5:1 $[OH^-]$:[Fe(III)] molar ratios. KMT suspensions were also treated with 0.75:1 and 1:1 $[OH^-]$:[Fe(III)] molar ratio solutions suspensions. The suspensions were centrifuged at 1000*g* for 10 min, and the solid phases were washed five times with deionized water. The modified clay minerals were freeze-dried, crushed, dried in an oven at 100 °C for 24 h, and stored in a desiccator. The intercalated clays prepared with $[OH^-]$:[Fe(III)] molar ratios 0.75:1, 1:1, 1.5:1, and 2:1 were identified by VT-OH/$Fe_{0.75:1}$, VT-OH/$Fe_{1:1}$, VT-OH/$Fe_{1.5:1}$, and VT-OH/$Fe_{2:1}$, respectively. Similarly, modified MTs were identified by MT-OH/$Fe_{0.75:1}$, MT-OH/$Fe_{1:1}$, and MT-OH/$Fe_{2:1}$.

The surface areas were obtained from BET measurements of N_2 adsorption isotherms using a Gemini 2375 V5.00 instrument from Micromeritics Instr. Corp. The pore volume was determined at a P/P_0 ratio of 0.95, while the micropore volumes were determined by the *t*-plot method (*31*). The basal spacing of K^+-saturated and Fe(III)-intercalated clays was estimated by X-ray diffraction using a Siemens D-5000 diffractometer. The iron contents in KVT, KMT, and intercalated clay minerals were determined in order to assess the amount of Fe(III) incorporated in the modified materials. These analyses were performed by treating 30 mg of the samples with 2.5 mL of 5% (v/v) HCl solution for 6 h. The supernatant phase was separated by centrifugation. This extraction was repeated five times, and the supernatant phases were combined for further Fe determination by flame atomic absorption spectrometry using a Perkin-Elmer 703 spectrometer. The iron content was also determined in the materials after the adsorption/desorption experiments performed with AT.

Adsorption and Desorption Experiments. Adsorption of AT, DEA, DIA, or ATOH was performed using the batch equilibration approach. Thirty milligrams (±0.1 mg) of each adsorbent was weighed in seven glass vials with a capacity of 4 mL. Next, 3.00 mL of the solution containing one of the studied compounds was added to the respective glass vial. The solute concentrations were 0.050, 0.075, 0.100, 0.250, 0.500, 0.750, and 1.00 mg L^{-1}. The vials were closed, protected from light, and kept under gentle agitation for 24 h in an orbital shaker programmed at 140 rpm. In parallel, five standards with concentrations between 0.0050 and 1.00 mg L^{-1}, together with the blank solution, were submitted exactly to the same procedure used for the adsorption experiments. After the 24 h of contact time, the pH of the suspensions was measured and the solid phases were separated by centrifugation for 15 min at 2600*g*. Afterward, 2.70 mL of the supernatant was withdrawn and filtered through 0.45 μm Durapore membrane Millex from Millipore. These solutions were buffered with a suitable volume of 1.0 mol L^{-1} ammonium acetate buffer (pH 4.5), and the concentrations of AT, DEA, DIA, and ATOH were determined by HPLC, using isocratic elution with a mobile phase consisting of 65% (v/v) 2.5 mmol L^{-1} ammonium acetate buffer and 35% (v/v) ACN. The wavelengths used for detection of AT, DEA, DIA, and ATOH were 220, 214, 214, and 236 nm, respectively. Under these conditions, the detection limits were 0.5 μg L^{-1} for AT, DEA, and DIA and 1.0 μg L^{-1} for ATOH.

The desorption experiments were performed by adding 2.70 mL of deionized water to the glass vials containing the adsorbing material and the remaining 0.30 mL of the herbicide or metabolite solution. The vials were protected from light and shaken for 24 h in an orbital shaker at 140 rpm. The desorption time of 24 h was based on Konstantinou et al. (*21*), who verified that desorption equilibrium is reached after 6 h for similar adsorbent materials. The suspensions were centrifuged, and the supernatant phase was treated as in the adsorption experiments and analyzed by the HPLC method.

Finally, 0.75 mL of ACN was added to the glass vials, which were closed and shaken for 30 min. The supernatant phases were carefully removed after centrifugation and a second desorption in ACN was carried out. ACN was chosen because it is a component of the mobile phase in the HPLC analyses. Both extracts were combined, diluted with an equal volume of 5.0 mmol L^{-1} ammonium acetate buffer, filtered, and analyzed by HPLC, as previously described.

To evaluate the possibility of reuse of the adsorbents, the materials used to study adsorption and desorption of AT were used for another adsorption experiment after an additional washing with 1.0 mL of acetone, to facilitate the drying of the adsorbent prior to reuse.

Data Treatment. Adsorption data were treated by the linearized Freundlich equation:

$$\log\left(\frac{x}{m}\right) = \log K_f + \left(\frac{1}{n}\right)\log C \qquad (1)$$

where x/m is μmol of AT, or metabolite, adsorbed per gram of soil; C is the solution concentration of the herbicide or metabolite; and K_f and $1/n$ are empirical constants related to adsorption.

RESULTS AND DISCUSSION

Adsorbents Characterization. Table 1 shows the basal spacing d(001) values of KVT, KMT, and their intercalated materials. The d(001) values for KVT and KMT materials are in reasonable agreement with the values reported in the literature of 10.0 and 11.6 Å for KVT and KMT, respectively (*32*). For iron-modified VT, the d(001) value was 14.5 Å, which is close to the value of 14 Å found by Del-Rey-Perez-Caballero and Poncelet (*33*) for Al-modified VT. The basal spacing of iron-modified MT was systematically larger than observed for VT (**Table 1**), which is a consequence of the layer charge of KMT that allows the separation between layers to occur at larger dimensions in aqueous medium, producing materials with especially interesting swelling properties (*32*). The $[OH^-]$:[Fe(III)] molar ratios did not affect the basal spacing of both VT or MT.

Table 1. Basal Spacing d(001), BET Surface Area, and Pore and Micropore Volumes of the Adsorbents

sample	d(001) (Å)	BET ($m^2\ g^{-1}$)	pore volume ($\mu L\ g^{-1}$)	micropore volume ($\mu L\ g^{-1}$)
KVT	10.8	31.4	14	2.1
VT-OH/$Fe_{0.75:1}$	14.5	48.8	21	4.0
VT-OH/$Fe_{1:1}$	14.5	43.1	19	3.5
VT-OH/$Fe_{1.5:1}$	15.1	50.4	22	3.7
VT-OH/$Fe_{2:1}$	14.5	52.1	22	3.6
KMT	13.0	228	97	1.9
MT-OH/$Fe_{0.75:1}$	16.6	246	104	0.7
MT-OH/$Fe_{1:1}$	15.8	270	116	5.4
MT-OH/$Fe_{2:1}$	16.4	246	105	11.7

Table 2. Iron Contents[a] of KVT, KMT, and Modified Clay Minerals without Use and after Being Used Twice in Experiments of AT Adsorption

sample	without use (%)	first use (%)	second use (%)
KVT	4.0 ± 0.1		
VT-OH/$Fe_{0.75:1}$	11.5 ± 0.6	11.5 ± 0.5	11.6 ± 0.3
VT-OH/$Fe_{1:1}$	11.4 ± 0.1	11.0 ± 0.8	10.5 ± 0.4
VT-OH/$Fe_{1.5:1}$	10.8 ± 0.5	10.8 ± 0.1	10.4 ± 0.1
VT-OH/$Fe_{2:1}$	10.7 ± 0.6	10.3 ± 0.2	7.6 ± 0.3
KMT	0.60 ± 0.06		
MT-OH/$Fe_{0.75:1}$	3.55 ± 0.07	3.41 ± 0.06	3.31 ± 0.03
MT-OH/$Fe_{1:1}$	3.4 ± 0.2	3.6 ± 0.1	3.47 ± 0.08
MT-OH/$Fe_{2:1}$	3.4 ± 0.1	3.5 ± 0.1	3.52 ± 0.08

[a] The results are the average of triplicates of experiments.

A significant increase in the pore volume and BET surface area was observed for VT-related materials after the incorporation of the polycations (**Table 1**). Conversely, only a small increase in the values of textural parameters was observed for MT materials. The different $[OH^-]$:[Fe(III)] molar ratios studied did not affect the pore volume and BET surface area of both intercalated clay minerals. Hydrolysis of Fe(III) decreases the charge of the polycation, leading to the precipitation. Because of the low charge, more pillar species are necessary to neutralize the CEC, and the interlayer space can be stuffed with pillars leaving no significant pore volume, with the final product resembling a mixed oxide (*34*). Nevertheless, a significant increase in the micropore volume was observed for the intercalated clays, except for MT-OH/$Fe_{0.75:1}$, for which this parameter decreased in comparison to KMT (**Table 1**).

The iron contents of KVT and KMT related materials are shown in **Table 2**. The amounts of iron incorporated in VT-OH/$Fe_{0.75:1}$ and VT-OH/$Fe_{1:1}$ are approximately 11.5%, implying an increment of 7.5% in comparison to KVT. For VT-OH/$Fe_{1.5:1}$ and VT-OH/$Fe_{2:1}$, an increase of approximately 6.7% was achieved. The lower incorporation of Fe(III) species for the suspensions with higher molar ratios may be explained by the larger polymeric species created in these suspensions (*35*), which may hinder the access of additional polymeric molecules to the interlayer space of the clay mineral, especially for VT, which has a limited increase of basal spacing (*32*). The iron content of KMT was around 0.6%, increasing about 3% for the three modified materials. The ratio of Fe(III) to the mass of VT and MT in the starting suspension was 10 mmol g^{-1}, so that the differences of iron content between the modified and the K^+ saturated materials are consistent with their CEC values of 1.17 and 0.59 mmol g^{-1} for KVT and KMT, respectively.

Adsorption onto VT. The adsorption curves of AT on KVT and related modified VTs are presented in **Figure 1A**. The initial concentrations of AT were between 0.050 and 1.0 mg L^{-1},

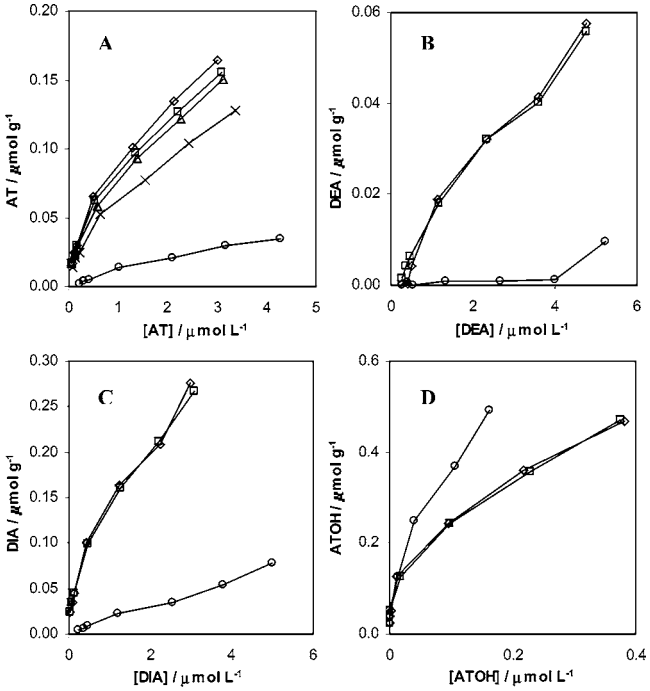

Figure 1. Adsorption curves of AT (**A**), DEA (**B**), DIA (**C**), and ATOH (**D**) onto KVT (○) and Fe(III)-hydroxy-intercalated clay minerals VT-OH/$Fe_{0.75:1}$ (◇), VT-OH/$Fe_{1:1}$ (□), VT-OH/$Fe_{1.5:1}$ (△), and VT-OH/$Fe_{2:1}$ (×).

which correspond to 0.232 and 4.64 μmol L^{-1}, respectively. Weak interactions between KVT and AT were observed, resulting in maximum removal percentages of only about 10%. For the materials VT-OH/$Fe_{0.75:1}$, VT-OH/$Fe_{1:1}$, and VT-OH/$Fe_{1.5:1}$, the removal percentages were between 75 and 33% for the lowest and highest initial AT concentrations studied, while for the same concentration interval the VT-OH/$Fe_{2:1}$ material removed from 60 to 30% of AT initially present in solution. **Table 3** shows that K_f values for adsorption of AT onto the intercalated VT were of similar magnitudes, denoting the dominance of medium affinity sites, as observed by Matthes and Kahr (*22*) for Na-rich bentonite. A significant increase in the K_f is observed in comparison to KVT, as well as in comparison to soil samples (*6*, *36*, *37*). The decrease of 1/*n* values (**Table 3**) for intercalated VT is in agreement with the increase of heterogeneity of the adsorption sites that may occur as a consequence of intercalating.

Protonation of AT in the interlayer water of the clay minerals followed by electrostatic interaction of the AT cation by negative charges of the mineral surface is a possible mechanism that can explain the adsorption enhancement in the modified VT (*38*). A similar behavior has also been observed for other weakly basic pesticides (*16*). Low pH values enhance the adsorption of weak bases, with maximum adsorption occurring at pH values close to the pK_a of the conjugate acid, leading to adsorption processes governed by electrostatic interactions of the cationic species with the negative charges of the mineral surface. Additionally, protonated adsorbate species are liable to interact with the mineral surface by hydrogen bonding. The hypothesis of adsorption of protonated AT species to the intercalated VT is supported by the pH of the suspensions, which, after 24 h of contact time, were 3.61, 3.67, 3.68, 4.31, and 7.14 for VT-OH/$Fe_{0.75:1}$, VT-OH/$Fe_{1:1}$, VT-OH/$Fe_{1.5:1}$, VT-OH/$Fe_{2:1}$, and KVT, respectively. Although the suspension pH of the intercalated clays is higher than the pK_a of AT, which is around of 1.7 (*39*), the adsorption of the herbicide as a cation can be favored by the hydrolysis of the Fe(III) polycations by the interlayer waters of the clay minerals, leading to a local increase of acidity that is not assessed by only measuring the suspension pH. Thus, the clay surface and water molecules in the interlayers work as proton donors favoring protonation of AT, even if the pH of the bulk suspension is above the pK_a (*21*, *22*).

Adsorption of DEA, DIA, and ATOH onto KVT, VT-OH/$Fe_{0.75:1}$, and VT-OH/$Fe_{1:1}$ (**Figure 1B**−**D**, respectively) was investigated using initial concentrations between 0.050 and 1.0 mg L^{-1}. These concentration intervals, expressed in μmol L^{-1}, are 0.266−5.33 (DEA), 0.288−5.76 (DIA), and 0.254−5.08 (ATOH). The suspension pH after 24 h of contact time was similar to the pH values found in the AT adsorption study. Adsorption of DEA onto KVT was negligible but increased significantly in the intercalated materials, although to an extension much lower than observed for AT. An up stage trend is observed in adsorption of DEA on KVT, a behavior that may be related to cooperative adsorption (*32*), which is also observed for the intercalated VT in a lesser extension (**Figure 1B**). However, higher initial concentrations should have been studied to confirm this hypothesis. An averaged adsorption percentage of only 10% of DEA onto VT-OH/$Fe_{0.75:1}$ and VT-OH/$Fe_{1:1}$ (**Figure 1B**) was observed in the concentrations interval studied. The adsorption of DIA by the modified VT materials was also significantly enhanced in comparison to adsorption onto KVT.

Adsorption of DIA was higher than AT onto all VT materials studied. The K_f values for interaction between DIA and VT-OH/$Fe_{0.75:1}$ or VT-OH/$Fe_{1:1}$ were higher than those observed for AT (**Table 3**) but still denoted medium affinity. As observed for AT, the 1/*n* values decreased for the modified VT in comparison to KVT, suggesting that similar mechanisms govern the interaction of both AT and DIA with these clay minerals.

ATOH was easily adsorbed on both KVT and modified VT materials. Adsorption percentages higher than 90% were obtained (**Figure 1D**), implying that the studied material adsorbed much more ATOH than AT, DEA, and DIA. Conversely to the other compounds, ATOH was removed to a larger extent by KVT, reaching an adsorption percentage of 97% for the last point of the adsorption curve (**Figure 1D**). This strong affinity can be explained by the pK_a of ATOH, which is 5.15 (*39*), therefore, much higher than the pK_a of AT, DEA, and DIA. As a consequence, ATOH is much more easily protonated than these compounds under our experimental conditions. The higher adsorption of ATOH onto KVT in comparison to the intercalated materials may be related to the higher pH of the KVT suspension. Aluminol and silanol groups of edge surface of clay minerals are liable to the following acid−base equilibria (*40*):

$$SiOH_2^+ \rightarrow SiOH + H^+ \ (pK_1 < 2) \quad (2)$$

$$SiOH \rightarrow SiO^- + H^+ \ (pK_2 = 6-7) \quad (3)$$

$$AlOH_2^+ \rightarrow AlOH + H^+ \ (pK_1 = 5-7.5) \quad (4)$$

$$AlOH \rightarrow AlO^- + H^+ \ (pK_2 = 8-10) \quad (5)$$

Because the pH of the KVT suspension is close to 7, the equilibrium (3) may have a key role in the formation of edge negative charges on the mineral surface, a process that is less likely to occur with the intercalated materials because of the lower pH of their suspensions. These negative charges at the edge surface facilitate the interaction with ATOH by hydrogen bonding, a mechanism that seems to be favored in the KVT material. The predominance of specific site adsorption in both,

Table 3. Adsorption and Desorption Freundlich Parameters for Interaction between AT, ATOH, DIA, and DEA with VT Materials

	adsorption			desorption		
material	K_f (μmol$^{1-1/n}$ L$^{1/n}$ kg^{-1})	1/*n*	*r*	K_f (μmol$^{1-1/n}$ L$^{1/n}$ kg^{-1})	1/*n*	*r*
			AT			
VT-OH/Fe$_{0.75:1}$	83 ± 4	0.54 ± 0.01	0.999	166 ± 12	0.85 ± 0.03	0.996
VT-OH/Fe$_{1:1}$	78 ± 4	0.61 ± 0.04	0.992	145 ± 13	0.86 ± 0.05	0.990
VT-OH/Fe$_{1.5:1}$	78 ± 2	0.57 ± 0.01	0.999	132 ± 6	0.82 ± 0.02	0.999
VT-OH/Fe$_{2:1}$	62 ± 3	0.63 ± 0.03	0.996	135 ± 13	0.96 ± 0.04	0.995
KVT	10.5 ± 0.7	0.90 ± 0.05	0.992			
			ATOH			
VT-OH/Fe$_{0.75:1}$	713 ± 98	0.43 ± 0.04	0.987	956 ± 44	0.47 ± 0.02	0.998
VT-OH/Fe$_{1:1}$	676 ± 31	0.43 ± 0.02	0.998	956 ± 44	0.48 ± 0.02	0.999
KVT	(1.2 ± 0.1) × 10^3	0.51 ± 0.03	0.997	(1.48 ± 0.03) × 10^3	0.58 ± 0.01	0.999
			DIA			
VT-OH/Fe$_{0.75:1}$	141 ± 3	0.58 ± 0.02	0.998	144 ± 6	0.71 ± 0.03	0.997
VT-OH/Fe$_{1:1}$	141 ± 3	0.56 ± 0.01	0.999	141 ± 3	0.69 ± 0.02	0.998
KVT	16.6 ± 0.8	0.93 ± 0.04	0.994			
			DEA			
VT-OH/Fe$_{0.75:1}$	17 ± 1	0.75 ± 0.06	0.994			
VT-OH/Fe$_{1:1}$	12.9 ± 0.9	0.96 ± 0.05	0.993			
KVT	0.45 ± 0.10	0.8 ± 0.2	0.87			

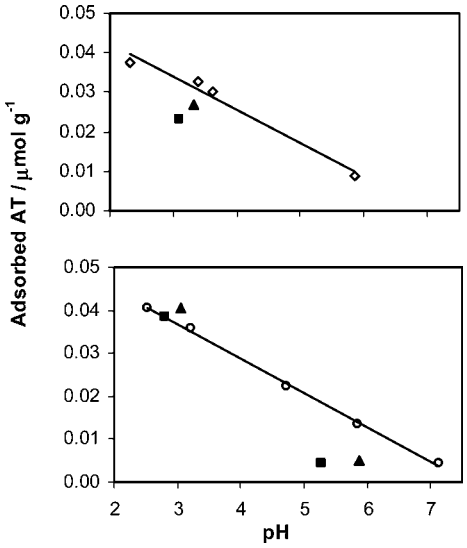

Figure 2. Influence of pH on the adsorption of AT onto KVT (○) and VT-OH/Fe$_{0.75:1}$ (◇) in medium of 0.01 (▲) or 0.1 (■) mol L^{-1} KCl. Initial concentration of AT = 0.046 μmol g^{-1}.

KVT and intercalated VT, is in agreement with the fact that the 1/*n* values (**Table 3**) were not significantly affected by the intercalating process.

The influence of pH and ionic strength on the adsorption of AT onto KVT and VT-OH/Fe$_{0.75:1}$ was investigated (**Figure 2**) adding suitable volumes of 0.1 mol L^{-1} HCl, KOH or 1.0 mol L^{-1} KCl to the clay mineral suspension. The adsorption onto both clay materials increases with the lowering of pH, confirming the hypothesis that adsorption occurs through electrostatic attractions mechanisms involving the protonated species of AT. It is interesting to notice that at pH 2.5, KVT adsorbs AT at a greater extension than VT-OH/Fe$_{0.75:1}$ (**Figure 2**), suggesting that low pH has a similar effect of intercalating, at least if the proposal is to improve adsorption capacity of the clay minerals for weakly basic compounds. The influence of pH was also studied with the intercalated clays VT-OH/Fe$_{1:1}$, VT-OH/Fe$_{1.5:1}$, and VT-OH/Fe$_{2:1}$, which had a similar behavior to the one described for VT-OH/Fe$_{0.75:1}$. At a pH of around 3.0, the influence of ionic strength is small, but it seems to decrease the adsorption of AT onto VT-OH/Fe$_{0.75:1}$, probably by competition of K^+ with protonated AT for anionic sites of clay mineral surface. For KVT, this competition at low pH seems to be less intense (**Figure 2**), although at a pH between 5 and 6 the competition increases significantly and the presence of 0.01 or 0.10 mol L^{-1} KCl decreases the adsorption of AT onto KVT.

Desorption from VT. Figure 3 shows the desorption isotherms of AT, DIA, and ATOH, while **Table 3** shows the K_f and 1/*n* parameters for these experiments. Desorption of DEA was not studied due to its low adsorption values on KVT and modified VT. The desorption isotherm of AT was approximately linear, resulting in desorption percentages between 28 and 40% for the modified clay minerals (**Table 4**). Desorption of DIA from VT-OH/Fe$_{0.75:1}$ and VT-OH/Fe$_{1:1}$ was undistinguishable, varying from 22 to 36% of the amount initially adsorbed. The high desorption percentages of AT and DIA suggest the occurrence of weak binding or attraction by physical forces, in agreement with the hypothesis of electrostatic interactions of AT, DEA, and DIA with the clay surface. The significant difference between the water solubility of AT (70 mg L^{-1}) and DIA (650 mg L^{-1}) seems to have no influence on the desorption of these compounds from VT-OH/Fe$_{0.75:1}$ and VT-OH/Fe$_{1:1}$. Conversely, desorption of ATOH from VT-OH/Fe$_{0.75:1}$, VT-OH/Fe$_{1:1}$, and VT-OH/Fe$_{1.5:1}$ was much less intense than AT and DIA (**Figure 3C**), with a maximum percentage of only 3% for the three clay materials studied (**Table 4**). The K_f values confirm the following desorption order: AT ∼ DIA > ATOH.

Desorption percentages of AT in ACN (**Table 4**) were between 60 and 40% of the initially adsorbed amount of herbicide in the first and last point of adsorption isotherm. Up to the initial concentration of 0.100 mg L^{-1} (used in the adsorption experiment), desorption was almost quantitative if one accounts for the sum of desorbed amounts in water and ACN. The total desorption percentage decreases as the concentration of AT increases, indicating that a small fraction of AT can be irreversibly adsorbed to the modified clays (at least in the time scale of the experiments). The chromatograms did not show the formation of DEA and DIA (usually resulting from biotic degradation), as well as ATOH. AT could have been partially hydrolyzed to ATOH, which is strongly retained by the modified clays, although Wang et al. (*41*) demonstrated that formation of ATOH occurs only after 3 days and a pH below 3.65. However, the possibility of AT hydrolysis should not be

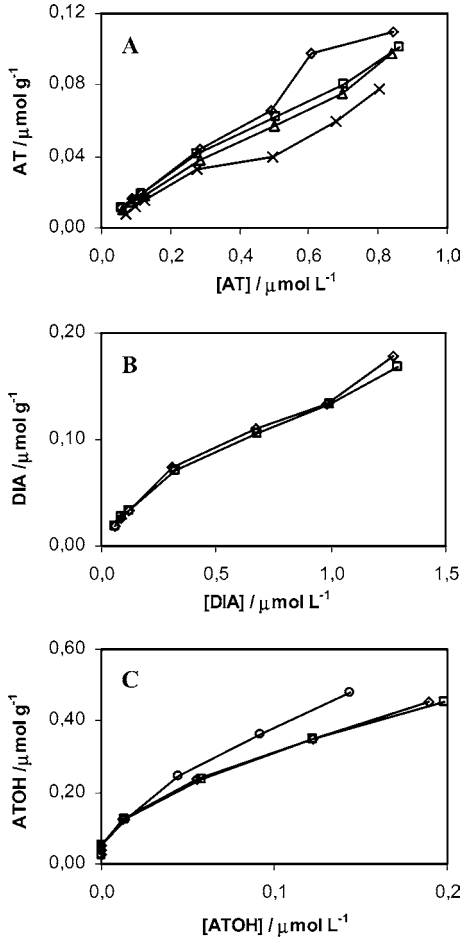

Figure 3. Desorption curves of AT (**A**), DIA (**B**), and ATOH (**C**) from modified VT-OH/$Fe_{0.75:1}$ (◇), VT-OH/$Fe_{1:1}$ (□), VT-OH/$Fe_{1.5:1}$ (△), and VT-OH/$Fe_{2:1}$ (×). Desorption from KVT (○) was studied only for ATOH.

Table 4. Desorption[a] of AT, DIA, and ATOH from KVT, VT-OH/$Fe_{0.75:1}$, VT-OH/$Fe_{1:1}$, VT-OH/$Fe_{1.5:1}$, and VT-OH/$Fe_{2:1}$ in Water and ACN

	AT (%)		DIA (%)		ATOH (%)	
sample	water	ACN	water	ACN	water	ACN
KVT					0–3	79–68
VT-OH/$Fe_{0.75:1}$	28–28	67–37	22–35	74–62	0–3	29–29
VT-OH/$Fe_{1:1}$	29–31	61–37	23–37	77–62	0–3	26–29
VT-OH/$Fe_{1.5:1}$	32–30	57–36				
VT-OH/$Fe_{2:1}$	41–31	63–32				

[a] The results are the average of duplicates of experiments and express the removal of the preadsorbed AT, DIA, or ATOH between the first and the last point of the desorption curves.

ruled out, since the adsorption and desorption experiments spent 48 h, additionally due to the fact that the pH of the interlayer water may be lower than 3.65, favoring the formation of ATOH.

The results of this work show that natural and intercalated VTs are not suitable materials to be used with the proposal of protecting surface and groundwaters from contamination with AT and its metabolites DEA and DIA. Only ATOH is strongly adsorbed, with a low degree of desorption. Nevertheless, because the adsorption of AT onto the intercalated VT is partially reversible, these materials have great potentiality for use in formulations that provide controlled release of AT in soils.

Adsorption onto MT. Adsorption percentages of AT were very high onto all materials (**Table 5**). Adsorption on KMT was stronger than on KVT, a fact that is related to the higher surface area and pore volume of the former (**Table 1**), implying

Table 5. Adsorption[a,b] of AT, DEA, DIA, and ATOH onto KMT, MT-OH/$Fe_{0.75:1}$, MT-OH/$Fe_{1:1}$, and MT-OH/$Fe_{2:1}$

sample	AT	DEA	DIA	ATOH
KMT	>99.5–99	72–64	>99.5–99	>99.5
MT-OH/$Fe_{0.75:1}$	>99.5	>99.5–94	>99.5	>99.5
MT-OH/$Fe_{1:1}$	>99.5	>99.5–95	>99.5	>99.5
MT-OH/$Fe_{2:1}$	>99.5	>99.5–95	>99.5	>99.5

[a] The results are the average of duplicates of experiments and express the percentages of adsorption of AT, DEA, DIA, or ATOH between the first and the last point of the adsorption curves. [b] The removal, >99.5%, was based on the detection limit of the HPLC technique.

an enhanced availability and accessibility of adsorption sites. The surface charge densities estimated as the ratio between the CEC and the BET surface area are 0.0373 and 0.00259 mmol m^{-2} for KVT and KMT, respectively. The stronger adsorption on KMT, which has a lower charge density, suggests that triazines can be adsorbed as neutral molecules by van der Waals forces and hydrogen bonding. This finding is in agreement with Barriuso et al. (*42*) who reported a decrease in the affinity of smectites for AT with the increase of CEC and surface charge density, concluding that physical sorption and hydrogen bonding are important mechanisms of AT retention. The adsorption of DIA and ATOH onto KMT and modified MT was analogous to that observed for AT; that is, the removal was almost quantitative and the solution concentrations of both compounds were smaller than the detection limit of the analytical method.

Because of the nearly complete adsorption of AT, DIA, and ATOH from water by KMT and intercalated MT, Freundlich parameters can only be calculated for DEA. The averaged adsorption percentage of DEA onto KMT was 70% ($K_f = 209 \pm 5$ $\mu mol^{1-1/n}$ $L^{1/n}$ kg^{-1}; $1/n = 0.91 \pm 0.02$) but increased significantly for MT-OH/$Fe_{0.75:1}$, MT-OH/$Fe_{1:1}$, and MT-OH/$Fe_{2:1}$, reaching values between 95 and 99.5%, with K_f values between $(1.3 \pm 0.1) \times 10^3$ (MT-OH/$Fe_{2:1}$) and $(1.5 \pm 0.2) \times 10^3$ $\mu mol^{1-1/n}$ $L^{1/n}$ kg^{-1} (MT-OH/$Fe_{1:1}$). The increase of K_f was followed by a decrease in $1/n$, suggesting that the adsorption enhancement is associated with the increase of heterogeneity and site specific interactions. This means that MT materials were much more efficient than VT to remove DEA from aqueous solutions.

Desorption from MT. The removal of previously adsorbed AT from MT-OH/$Fe_{0.75:1}$, MT-OH/$Fe_{1:1}$, and MT-OH/$Fe_{2:1}$ in aqueous solution was not measurable up to the tube corresponding to the initial concentration of 1.0 mg L^{-1} AT. Desorption percentages between 1 and 3% were observed for the tubes with an initial AT concentration of 10 mg L^{-1}. As observed for AT, no detectable concentrations of DIA and ATOH were verified in the desorption study, confirming that interactions of AT, DIA, and ATOH with MT materials are irreversible in the time scale of the experiment. This behavior cannot be explained by van der Waals forces or normal hydrogen bonding, which are relatively weak, leading to reversible adsorption (*42*). A possible explanation is the occurrence of strong hydrogen bonds between the AT molecules and the polarized water molecules coordinated with interlayer cations of high ionic potential such as the Fe(III) (*32*, *43*). The large surface area and pore volume of MT materials can also explain the irreversible sorption of AT, DIA, and ATOH because of slow diffusion of compounds through the mineral particles (*44*).

Desorption of preadsorbed DEA was close to 5% for MT-OH/$Fe_{0.75:1}$, MT-OH/$Fe_{1:1}$, and MT-OH/$Fe_{2:1}$, while for KMT, the desorption percentage was around 30% in the last point of the curve (which corresponds to initial DEA concentration of

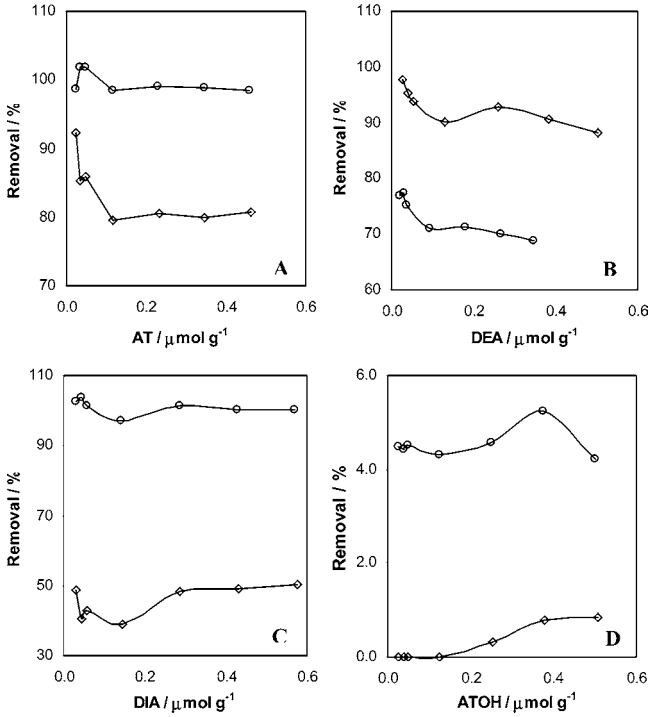

Figure 4. Desorption percentages of AT (**A**), DEA (**B**), DIA (**C**), and ATOH (**D**) from KMT (○) and MT-OH/$Fe_{0.75:1}$ (◇) in ACN.

1.0 mg L^{-1}). Desorption K_f values for KMT were 186 ± 4 $\mu mol^{1-1/n}$ $L^{1/n}$ kg^{-1}, while for MT-OH/$Fe_{0.75:1}$, MT-OH/$Fe_{1:1}$, and MT-OH/$Fe_{2:1}$, the K_f values were (9.5 ± 0.8) × 10^2, (9 ± 1) × 10^2, and (8.7 ± 0.4) × 10^2 $\mu mol^{1-1/n}$ $L^{1/n}$ kg^{-1}, respectively. These values indicate that DEA is strongly retained in the solid phase under desorption conditions.

Desorption percentages from MT-OH/$Fe_{0.75:1}$ and KMT in ACN are shown in **Figure 4**. Desorption from MT-OH/$Fe_{1:1}$ and MT-OH/$Fe_{2:1}$ was indistinguishable from MT-OH/$Fe_{0.75:1}$ and was not shown in **Figure 4**. Recoveries of AT and DIA from KMT were close to 100%. For DEA, desorption in ACN was close 70% of the initially adsorbed amount of metabolite. Because 30% of DEA was desorbed in water, the sum of amounts desorbed in water and ACN leads to quantitative removal. On the other hand, only 4.5% of ATOH was desorbed, confirming the strong bonding of this metabolite with KMT. Desorption of all compounds from MT-OH/$Fe_{0.75:1}$ was systematically smaller than observed from KMT (**Figure 4**), with the ATOH exhibiting the strongest interaction with the intercalated clay minerals. The results of the desorption studies in water and ACN allow one to depict the following affinity order for both KMT and its intercalated forms: ATOH > DIA > AT > DEA.

Recyclability. These experiments were carried out only for AT. A significant attenuation of the adsorption performance was observed for all intercalated VTs in the second adsorption cycle (**Table 6**). The AT amount adsorbed in the first cycle was removed with water and ACN. The K_f values decreased to the range between 40 and 50 $\mu mol^{1-1/n}$ $L^{1/n}$ kg^{-1}. The suspension pH of VT-OH/$Fe_{0.75:1}$, VT-OH/$Fe_{1:1}$, and VT-OH/$Fe_{1.5:1}$ after the second adsorption step was 4.25, which is about 0.6 units higher than observed at the end of the first adsorption step. Because the protonation of AT seems to be the key factor governing the adsorption effectiveness onto VT materials, the performance decay may be attributed to the pH increase.

The equilibrium pH of the intercalated MT increased about 0.5 units after the second adsorption step, but different from VT, the adsorption effectiveness was not affected. For KMT material, the pH values were 6.3 and 6.4 after the first and second adsorption steps and, as observed for the intercalated materials, the adsorption performance was not affected. These properties suggest that the intercalated MT materials can be reutilized without the loss of adsorption properties (at least for the materials prepared from the commercial K10 MT), making them interesting materials for applications such as wastewater treatment.

Table 6. Recyclability of KMT and Intercalated VT and MT after the Use for AT Removal

sample	AT removal (%),[a,b] first use	AT removal (%),[a,b] second use
VT-OH/$Fe_{0.75:1}$	77–35	54–21
VT-OH/$Fe_{1:1}$	74–34	55–19
VT-OH/$Fe_{1.5:1}$	74–33	55–19
VT-OH/$Fe_{2:1}$	59–28	33–17
KMT	>99.5–99	>99.5–99
MT-OH/$Fe_{0.75:1}$	>99.5	>99.5
MT-OH/$Fe_{1:1}$	>99.5	>99.5
MT-OH/$Fe_{2:1}$	>99.5	>99.5

[a] The results are the average of duplicates of experiments and express the percentages of adsorption of AT between the first and the last point of the adsorption curves. [b] The removal, >99.5%, was based in the detection limit of the HPLC technique.

LITERATURE CITED

(1) Graymore, M.; Stagnitti, F.; Allinson, G. Impacts of atrazine in aquatic ecosystems. *Environ. Int.* **2001**, *26*, 483−495.

(2) Moorman, T. B.; Jayachandran, K.; Reungsang, A. Adsorption and desorption of atrazine in soils and subsurface sediments. *Soil Sci.* **2001**, *166*, 921−929.

(3) Wood, M.; Issa, S.; Albuquerque, M.; Johnson, A. C. Spatial variability in herbicide degradation in the subsurface environment of a groundwater protection zone. *Pest Manage. Sci.* **2001**, *58* (2), 3−9.

(4) Stevenson, F. J. *Humus Chemistry, Genesis, Composition, Reactions*, 2nd ed.; John Wiley & Sons: New York, 1994.

(5) Loiseau, L.; Barriuso, E. Characterization of the atrazine's bound (nonextractable) residues using fractionation techniques for soil organic matter. *Environ. Sci. Technol.* **2002**, *36*, 683−689.

(6) Mersie, W.; Seybold, C. Adsorption and desorption of atrazine, deethylatrazine, deisopropylatrazine and hydroxyatrazine on Levy Wetland Soil. *J. Agric. Food Chem.* **1996**, *44*, 1925−1929.

(7) Panshin, S. Y.; Carter, D. S.; Bayless, E. R. Analysis of atrazine and four degradation products in the pore water of the vadose zone, Central Indiana. *Environ. Sci. Technol.* **2000**, *34*, 2131−2137.

(8) Gamble, D. S.; Khan, S. U. Atrazine in mineral soil: Chemical species and catalysed hydrolysis. *Can. J. Chem.* **1991**, *70*, 1597−1603.

(9) Monteiro, R. T. R.; Queiroz, B. P. V.; Cella, A. C. Distribution of ^{14}C-atrazine residues in humus fractions of a Brazilian soil. *Chemosphere* **1999**, *39* (2), 293−301.

(10) Berg, M.; Müller, S. R.; Schwarzenbach, R. P. Simultaneous determination of triazines including atrazine and their major metabolites hydroxyatrazine, deethylatrazine, and deisopropylatrazine in Natural Waters. *Anal. Chem.* **1995**, *67*, 1860−1865.

(11) Townsend, M. A.; Young, D. P. Atrazine and its metabolites as indicators of stream-aquifer interactions in Kansas, USA. *Int. J. Environ. Anal. Chem.* **2000**, *78*, 9−23.

(12) Carabias-Martínez, R.; Rodríguez-Gonzalo, E.; Herrero-Hernández, E.; Sánchez-San Román, F. J.; Flores, M. G. P. Determination of herbicides and metabolites by solid-phase extraction and liquid chromatography. Evaluation of pollution due to herbicides in surface and groundwaters. *J. Chromatogr. A* **2002**, *950*, 157−166.

(13) dos Santos, L. B. O.; Abate, G.; Masini, J. C. Determination of atrazine using square wave voltammetry with the hanging mercury drop electrode (HMDE). *Talanta* **2004**, *62*, 667−674.
(14) Bergaya, F.; Lagaly, G. Surface modifications of clay minerals. *Appl. Clay Sci.* **2001**, *19*, 1−3.
(15) Lagaly, G. Pesticide-clay interactions and formulations. *Appl. Clay Sci.* **2001**, *18*, 205−209.
(16) Celis, R.; Hermosín, M. C.; Carrizosa, M. J.; Cornejo, J. Inorganic and organic clays as carriers for controlled release of the herbicide hexazinone. *J. Agric. Food Chem.* **2002**, *50*, 2324−2330.
(17) Carrizosa, M. J.; Calderón, M. J.; Hermosín, M. C.; Cornejo, J. Organosmectites as sorbent and carrier of the herbicide bentazone. *Sci. Total Environ.* **2000**, *247*, 285−293.
(18) Prost, R.; Yaron, B. Use of modified clays for controlling soil environmental quality. *Soil Sci.* **2001**, *166* (12), 880−895.
(19) Michot, L. J.; Pinnavaia, T. J. Adsorption of chlorinated phenols from aqueous solution by surfactant-modified pillared clays. *Clays Clay Miner.* **1991**, *39* (6), 634−641.
(20) González-Pradas, E.; Villafranca-Sánchez, M.; Del Rey-Bueno, F.; Ureña-Amate, M. D.; Socías-Viciana, M.; Fernández-Pérez, M. Removal of diquat and deisopropylatrazine from water by montmorillonite-(Ce or Zr) phosphate cross-linked compounds. *Chemosphere* **1999**, *39* (3), 455−466.
(21) Konstantinou, I. K.; Albanis, T. A.; Petrakis, D. E.; Pomonis, P. J. Removal of herbicides from aqueous solutions by adsorption on Al-pillared clays, Fe−Al pillared clays and mesoporous alumina aluminum phosphates. *Water Res.* **2000**, *34* (12), 3123−3136.
(22) Matthes, W.; Kahr, G. Sorption of organic compounds by Al and Zr-hydroxy-intercalated and pillared bentonite. *Clays Clay Miner.* **2000**, *48* (6), 593−602.
(23) Jiang, J. Q.; Cooper, C.; Ouki, S. Comparison of modified montmorillonite adsorbents. Part I: Preparation, characterization and phenol adsorption. *Chemosphere* **2002**, *47*, 711−716.
(24) Jiang, J. Q.; Zeng, Z. Q. Comparison of modified montmorillonite adsorbents. Part II: The effects of the type of raw clays and modifications conditions on the adsorption performance. *Chemosphere* **2003**, *53*, 53−62.
(25) Pinnavaia, T. J. Intercalated clay catalysts. *Science* **1983**, *220*, 365−371.
(26) Yang, R. T.; Cheng, L. S. Pillared clays and ion-exchanged pillared clays as gas adsorbents and as catalysts for selective catalytic reductions of NO. In *Access in Nanoporous Materials*; Pinnavaia, T. J., Thorpe, M. F., Eds.; Plenun Press: New York, 1995.
(27) Khalaf, H.; Bouras, O.; Perrichon, V. Synthesis and characterization of Al-pillared and cationic surfactant modified Al-pillared Algerian bentonita. *Microporous Mater.* **1997**, *8*, 141−150.
(28) Lenoble, V.; Bouras, O.; Deluchat, V.; Serpaud, B.; Bollinger, J. Arsenic adsorption onto pillared clays and iron oxides. *J. Colloid Interface Sci.* **2002**, *255*, 52−58.
(29) Abate, G.; Masini, J. C. Influence of pH and ionic strength on removal processes of a sedimentary humic acid in a suspension of vermiculite. *Colloids Surf., A* **2003**, *226*, 25−34.
(30) Hesse, P. R. *A Textbook of Soil Chemical Analysis*; John Murray Publishers: London, 1971.
(31) De Boer, J. H.; Lippens, B. C.; Linsen, B. G.; Broekhoff, J. C. P.; van den Heuvel, A.; Osinga, T. J. The *t*-curve of multimolecular N_2-adsorption. *J. Colloid Interface Sci.* **1966**, *21*, 405−414.
(32) McBride, M. B. *Environmental Chemistry of Soils*; Oxford University Press: New York, 1994.
(33) Del-Rey-Perez-Caballero, F. J.; Poncelet, G. Microporous 18 Å Al-pillared vermiculites: Preparation and characterization. *Microporous Mesoporous Mater.* **2000**, *37*, 313−327.
(34) Maes, N.; Heylen, I.; Cool, P.; Vansant, E. F. The relation between the synthesis of pillared clays and their resulting porosity. *Appl. Clay Sci.* **1997**, *12*, 43−60.
(35) Bandosz, T. J.; Cheng, K. Changes in acidity of Fe-pillared/delaminated smectites on heat treatment. *J. Colloid Interface Sci.* **1997**, *191*, 456−463.
(36) Krutz, J. L.; Senseman, S. A.; McInnes, K. J.; Zuberer, D. A.; Tierney, D. P. Adsorption and desorption of atrazine, deethylatrazine, deisopropylatrazine, and hydroxyatrazine in vegetated filter strip and cultivated soil. *J. Agric. Food Chem.* **2003**, *51*, 7379−7384.
(37) Abate, G.; Penteado, J. C.; Cuzzi, J. D.; Vitti, G. C.; Lichtig, J.; Masini, J. C. Influence of humic acid on adsorption and desorption of atrazine, hydroxyatrazine, deethylatrazine and deisopropylatrazine onto a clay rich soil sample. *J. Agric. Food Chem.* **2004**, *52*, 6747−6754.
(38) Mortland, M. M.; Raman, K. V. Surface acidity of smectites in relation to hydration, exchangeable cation, and structure. *Clays Clay Miner.* **1968**, *16*, 393−398.
(39) Vermeulen, N. M. J.; Apostolides, Z.; Potgieter, D. J. J. Separation of atrazine and some of its degradation products by high-performance liquid chromatography. *J. Chromatogr.* **1982**, *240*, 247−253.
(40) Schindler, P. W.; Stumm, W. The surface chemistry of oxides, hydroxides and oxide minerals. In *Aquatic Surface Chemistry*; Stumm, W., Ed.; Wiley: New York, 1987.
(41) Wang, Z.; Gamble, D. S.; Langford, C. H. Interaction of atrazine with Laurentian fulvic acid: Binding and hydrolysis. *Anal. Chim. Acta* **1990**, *232*, 181−188.
(42) Barriuso, E.; Laird, D. A.; Koskinen, W. C.; Dowdy, R. H. Atrazine desorption from smectites. *Soil Sci. Soc. Am. J.* **1994**, *58*, 1632−1638.
(43) Sawhney, B. L.; Singh, S. S. Sorption of atrazine by Al- and Ca-saturated smectite. *Clays Clay Miner.* **1997**, *45*, 333−338.
(44) Pignatello, J. J.; Xing, B. Mechanisms of slow sorption of organic chemicals to natural particles. *Environ. Sci. Technol.* **1996**, *30*, 1−11.

Received for review August 31, 2004. Revised manuscript received December 20, 2004. Accepted December 20, 2004. We are grateful to FAPESP and CNPq for financial support and fellowships.

JF048556J